ChemComm

COMMUNICATION

View Article Online
View Journal | View Issue

Cite this: *Chem. Commun.*, 2021, 57, 11060

Received 31st August 2021,
Accepted 28th September 2021

DOI: 10.1039/d1cc04870h

rsc.li/chemcomm

Expanding manganese(IV) aqueous chemistry: unusually stable water-soluble hexahydrazide clathrochelate complexes†

Sergii I. Shylin,[ab] James L. Pogrebetsky,[a] Alina O. Husak,[ac] Dmytro Bykov,[d] Andriy Mokhir,[e] Frank Hampel,[e] Sergiu Shova,[f] Andrew Ozarowski,[g] Elzbieta Gumienna-Kontecka[h] and Igor O. Fritsky *[ac]

Mn cage complexes are rare, and the ones successfully isolated in the solid state are not stable in water and organic solvents. Herein, we present the first report of mononuclear Mn clathrochelates, in which the encapsulated metal exists in the oxidation state +4. The complexes are extremely stable in the crystalline state and in solutions and show rich redox chemistry.

Clathrochelates, or cage compounds, constitute a special type of complexes containing a metal ion in a three-dimensional ligand cavity.[1] As encapsulated in the macropolycyclic cage, the coordinatively saturated metal ion is shielded to a great extent from various external factors, including effects of solvents and *exo*-coordination that precludes the occurrence of redox processes by inner-sphere mechanisms and ligand substitution reactions.[1] For this reason, clathrochelates often exhibit a number of unusual properties, for example, they frequently attain enormous chemical and electrochemical stability.

The typical geometry of clathrochelates as a rule is intermediate between trigonal antiprismatic and prismatic giving rise to unusual non-octahedral orbital splitting.[1,2] This results in non-typical spin states and configurations,[3] and may lead to efficient stabilization of unusual oxidation states of caged metals.[1–4]

We have recently reported unprecedentedly stable Fe(IV) clathrochelates which are based on the hexahydrazide cage ligand and formed in aqueous solution under atmospheric conditions.[2] We attribute this unusual stability of tetravalent Fe to the strong σ-donor ability of the macrobicyclic ligand providing six deprotonated hydrazide groups in combination with the metal ion shielding effect.[2] We also demonstrated that a long-lived low-spin Fe(V) (S = 1/2) species can be generated from the Fe(IV) cage complex in an aqueous solution both chemically and photochemically, and it acts as a catalytic intermediate in the photochemical water oxidation.[3]

In view of our recent work on high-valent Fe clathrochelates, we assumed that the hexahydrazide ligand environment can stabilize high oxidation states of other 3d-metals in a similar—and efficient—manner. Specifically, high-valent Mn complexes attract considerable interest as they often exhibit catalytic and photocatalytic activity in various redox processes, particularly, functioning as superoxide dismutase, Mn ribonucleotide reductase and photosystem II biomimetics.[5] Also, Mn(IV) species have been postulated as active intermediates in Mn-catalyzed oxidative transformations of various organic substrates and in water oxidation.[5a–d] On the other hand, Mn(IV) aqueous chemistry is prevailed by insoluble dioxide which forms readily in water, so that Mn(IV) complexes are not stable in aqueous media and undergo decomposition with precipitation of the dioxide.[6]

Unlike Fe and Co clathrochelates, Mn cage compounds are rather rare, and only a few are presented in the literature.[7,8] Mn(II) sarcophaginate and sepulchrate complexes have been synthesized by reactions of Mn^{2+} salts with the corresponding ligands,[7] while Mn(II) tris(dioximate) clathrochelates capped with boronic acid derivatives have been prepared by template synthesis.[8a,b] The main challenge in obtaining of Mn cage complexes is their solution instability. Thus, Mn(II) tris(dioximate) cages readily undergo solvolysis in water or alcohols to give H-bonded pseudoclathrochelates and, finally, monocapped compounds.[8b]

[a] *Department of Chemistry, Taras Shevchenko National University of Kyiv, 64, Volodymyrska Str., 01601 Kiev, Ukraine. E-mail: ifritsky@univ.kiev.ua*
[b] *Department of Chemistry – Ångström Laboratory, Uppsala University, PO Box 523, 75120 Uppsala, Sweden*
[c] *PBMR Labs Ukraine, Murmanska 1, 02094 Kiev, Ukraine*
[d] *National Center for Computational Sciences, Oak Ridge National Laboratory, Oak Ridge, TN 37831, USA*
[e] *Department of Chemistry and Pharmacy, Friedrich-Alexander-University Erlangen-Nürnberg, Nikolaus-Fiebiger-Str. 10, 91058 Erlangen, Germany*
[f] *"Poni Petru" Institute of Macromolecular Chemistry, Aleea Gr. Ghica Voda 41A, 700487 Iasi, Romania*
[g] *National High Magnetic Field Laboratory, Florida State University, Tallahassee, Florida 32310, USA*
[h] *Faculty of Chemistry, University of Wrocław, F. Joliot-Curie Str. 14, 50-383 Wrocław, Poland*

† Electronic supplementary information (ESI) available: cif files, experimental details, DFT calculations and supplementary figures. CCDC 1848625 and 2009519. For ESI and crystallographic data in CIF or other electronic format see DOI: 10.1039/d1cc04870h

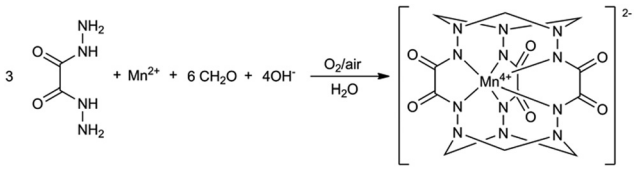

Scheme 1 Synthesis of Mn(IV) clathrochelate complexes.

Mn(III) sarcophagine complexes obtained by chemical or electrochemical oxidation of the corresponding Mn(II) cage complexes[7a,b] appeared to be stable only in strongly acidic aqueous solutions, while their parent Mn(II) species are even less stable undergoing hydrolysis or readily oxidizing to Mn(III).[7b]

In this paper we report the template synthesis of stable, water-soluble mononuclear Mn(IV) double capped clathrochelates based on a hexahydrazide cage ligand, which is formed as a result of atmospheric oxidation in aqueous solution (Scheme 1).

We succeeded to isolate two clathrochelates $(Ph_4As)_2[Mn^{IV}(L\text{-}6H)]\cdot 13.5H_2O$ (**1**) and $[Na_2(H_2O)_3Mn^{IV}(L\text{-}6H)]_n\cdot 4nH_2O$ (**2**) as dark green crystalline materials.

Both complexes are soluble in water, while **1** is also soluble in alcohols, acetone, acetonitrile, chloroform and dichloromethane. The UV-vis spectrum of aqueous solution of **1** indicates strong absorption in the visible region with distinct maxima at 658 nm ($\varepsilon = 3700\ M^{-1}\ cm^{-1}$) and 507 nm ($3000\ M^{-1}\ cm^{-1}$) assigned to the metal-to-ligand charge transfer resulting in an intense green color (Fig. S1, ESI†). UV-Vis control of the complex stability in aqueous solution during the period of 45 days revealed the absence of changes in positions of maxima and noticeable decay of spectral intensities (less than 4%) and only *ca.* 10% intensities decay on the 106th day (Fig. S2, ESI†).

Samples of **1** and **2** suitable for X-ray analysis were obtained as black crystals by slow evaporation of aqueous solutions at ambient conditions. Single crystal X-ray diffraction analysis revealed that the compound **1** crystallizes in the orthorhombic space group *Pbca*, and **2** in the triclinic space group $P\bar{1}$ (Tables S1–S5, ESI†). The structure of the clathrochelate complex dianion $[Mn^{IV}(L\text{-}6H)]^{2-}$ containing the encapsulated Mn^{4+} is shown in Fig. 1. The macropolycyclic ligand features the N-donor cage framework and two capping 1,3,5-triazacyclohexane fragments consisting of three five- and six six-membered alternating chelate rings. While the structure of **1** is ionic, **2** is a coordination polymer, so that the unit cells of **1** and **2** contain also the counter-cations ($AsPh_4^+$ and Na^+, respectively), guest water molecules, and water taking part in sodium cations coordination in **2** (Fig. S3–S7, ESI†).

The MnN_6-coordination geometry of the metal centers in **1** and **2** is intermediate between a trigonal prism (TP, distortion angle $\varphi = 0°$) and a trigonal antiprism, *i.e.*, octahedron (TAP, $\varphi = 60°$) with φ of 28.0° and 32.3° for **1** and **2**, respectively (Table S6, ESI†). As these values lie in the intermediate range of possible distortion angle (they are close to 30°) we used continuous shape measure (SHAPE 2.1 software)[9] to describe precisely the coordination geometry of the central ions. The calculated results (Table S7, ESI†) indicate that the geometry of

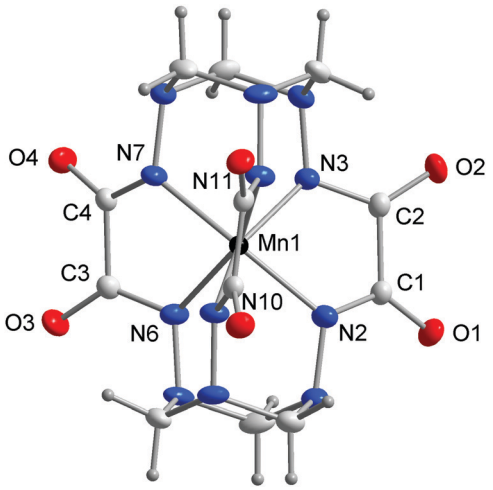

Fig. 1 General view of the clathrochelate complex anion $[Mn^{IV}(L\text{-}6H)]^{2-}$ in **1** with the atomic numbering scheme. Color scheme: black = Mn, red = O, blue = N, light grey = C, grey = H.

Mn^{4+} ion in **1** is viewed as trigonal-prismatic. However, the coordination geometry around the Mn atom in **2** is best described as distorted octahedral ($S_Q(P)$ values for octahedron and trigonal prism are 3.863 and 5.108, respectively). These conclusions are in line with larger distortion angle in **2** evidently caused by *exo*-coordination of sodium ions to the clathrochelate cation (Fig. S7, ESI†).

The Mn–N bond distances in **1** and **2** (1.970(3)–1.992(3) Å) are noticeably larger than those observed for the hexahydrazide Fe(IV) ($S = 1$) clathrochelates (1.915(5)–1.969(3) Å).[2] This is in line with general trend of late 3d-metal ions to decrease the ionic radius with increase of the atomic number[10] and is also conditioned by differences in 3d electronic configurations. The longer distances may be attributed to the decrease in electron density of the manganese(IV) core compared to iron(IV), that brings about less screening of the metal positive charge and thus larger repulsion with the ligands. At the same time *h* (the distance between the coordination polyhedron bases) and the bite angles are very close for Mn(IV) and Fe(IV) clathrochelates. Specifically, *h* for both Mn clathrochelates **1** and **2** and Fe complex with Ph_4As^+ cation are 2.39, 2.39 and 2.38 Å, respectively. Also, the bite angles exhibit very close values for both metals and are in the range of 78.51(1)–80.37(8)° for the Mn(IV) and 78.8(1)–80.8(2)° for the Fe(IV) complexes.[2]

The magnetic properties of **1** are shown in Fig. 2. The value of the effective magnetic moment, μ_{eff}, at 300 K of 3.874 μ_B is equal to the spin-only value for three unpaired electrons. The magnetic moment is constant in the range of 5–300 K, which indicates a high spin ground state of Mn(IV) ($S = 1.5$). Below 5 K, μ_{eff} slightly drops reaching 3.80 μ_B at 1.85 K (Fig. 2a). Such small and quite low-temperature drop of magnetic moment is indicative of insignificant ($<1\ cm^{-1}$) zero-field splitting. Interestingly, this is rather different from magnetic behavior of the iron(IV) clathrochelate which indicates significant decrease of magnetic moment already below 40 K with quite large zero-field splitting of *ca.* 23 cm^{-1}.[2] The experimental curve can be fitted

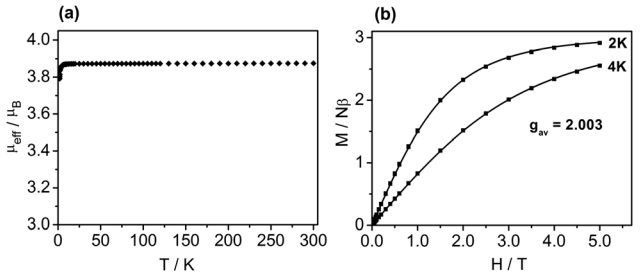

Fig. 2 (a) Temperature dependence of magnetic moment for the crystalline sample of **1**. (b) Field dependent magnetization data for the solid sample **1** at different temperatures.

with taking into account Zeeman splitting resulting in g = 2.000, and the observed drop of magnetic moment below 5 K is due to magnetization saturation (Fig. S8, ESI†). Attempts to introduce D and E parameters into the model did not result in any improvement of the fitting parameters and did not allow to obtain stable meaningful values.

In order to confirm the quartet ground state in **1**, a study of the field dependent magnetization was performed at 2 and 4 K (Fig. 2b). The measurements indicate that at 2 K the magnetization curve approaches saturation with M rising steeply to a value of 2.92 Nβ at 5 T. The magnetization data are excellently fitted using the appropriative Brillouin function resulting in g = 1.997 at 2 K and 2.009 at 4 K with S = 1.5.

The high-field EPR spectrum of **1** recorded at 10 K with microwave frequency of 388 GHz is presented in Fig. 3a. The resolution is quite poor because of large linewidth and small splitting due to the g anisotropy and zero-field splitting in the S = 1.5 state. The advantage of the high-field EPR in such cases is that spectra can be collected over a very large frequency range and the g values as well as the zero-field splitting parameters D and E can be reliably determined from the frequency dependencies of the features seen in the powder spectra (Fig. 3b).

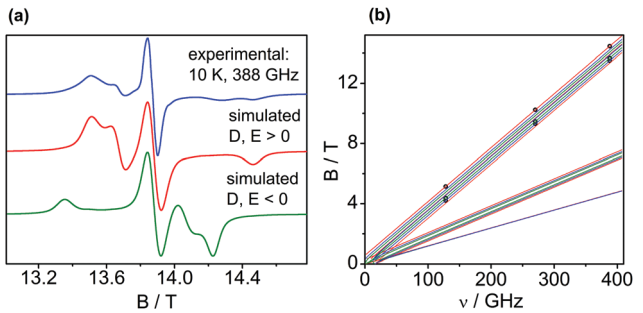

Fig. 3 (a) Top: HF EPR spectrum of **1** (powder) recorded at 10 K with the microwave frequency 388.0 GHz. Middle: Simulation with g_x = 1.998, g_y = 1.999, g_z = 1.9935, D = +0.259 cm^{-1}, E = +0.026 cm^{-1}. Bottom: Simulations with negative D and E. (b) The frequency dependencies of the EPR spectra recorded at 10 K. Circles: experimental points. The green, blue and red lines represent the resonance positions calculated at the X, Y and Z orientations, respectively. Fitting of these dependencies produced g_x = 1.998(1), g_y = 1.999(1), g_z = 1.9935(10), D = +0.259(2) cm^{-1}, E = +0.026(2) cm^{-1}. Note that only the high-field Z and only the low-field X, Y transitions are observed when D is positive.

Another advantage is the possibility to extract the sign of D, which came positive, in accordance with other manganese(IV) complexes.[11] Our density functional theory (DFT) calculations of the clathrochelate anion in **1** revealed the quartet ground state of manganese(IV), S = 1.5, and yielded the values $g_x = g_y$ = 1.998, g_z = 2.002, and D = +0.285 (see Fig. S9, ESI,† for details), which are in excellent agreement with the magnetochemical data and high-filed EPR experiments.

The cyclic voltammograms (CVs) of **1** in acetonitrile solution reveal a quasireversible one-electron oxidation process at $E_{1/2}$ = 0.05 V *vs.* Fc/Fc$^+$ with ΔE_p = 80 mV (Fig. 4a and Fig. S10, ESI†) which can be unambiguously assigned to the $Mn^{5+/4+}$ redox couple. It is followed by an irreversible feature at $E_{1/2}$ = 0.55 V with ΔE_p = 97–130 mV attributed to the $Mn^{6+/5+}$ redox couple (Fig. S11, ESI†). Another irreversible redox process observed at higher potential (0.74 V) may be due to either oxidative destruction of the complex or electrocatalytic oxidation of water traces. Scanning towards the negative potentials (down to −1.5 V *vs.* Fc/Fc$^+$) did not reveal any reduction events.

In aqueous solution, two quasireversible redox processes are registered as well (Fig. S12, ESI†), however, the one observed in the negative potential range (at $E_{1/2}$ = −0.17 V *vs.* NHE with ΔE_p = 86 mV) can be evidently assigned to the one-electron reduction to Mn^{3+} (Fig. S13, ESI†). At higher potentials, another redox wave is observed (at $E_{1/2}$ = 1.05 V *vs.* NHE with ΔE_p = 90 mV) which probably corresponds to the one-electron oxidation $Mn^{5+/4+}$ (Fig. 4b and Fig. S14, ESI†). The reduction and oxidation processes proved to be quasireversible for at least 20 cycles. The observed values of the redox potentials suggest efficient stabilization of the tetravalent oxidation state associated with strong σ-donor capacity of the deprotonated hydrazide groups,[12] robustness and high overall negative charge (−6) of the clathrochelate framework,[2,3] as well as smooth accessibility of higher oxidation states both in acetonitrile and aqueous media.

In this paper, the first genuine mononuclear manganese clathrochelate is reported. Importantly, our findings allow to overcome the problem of considerable instability of mononuclear manganese cage complexes reported to date, therefore, making it possible to exploit the possibilities to use them in various applications. While solid-state Mn(IV) is not surprising, the title compound is interesting because of its aqueous solubility and enormous stability in water. Even the most stable

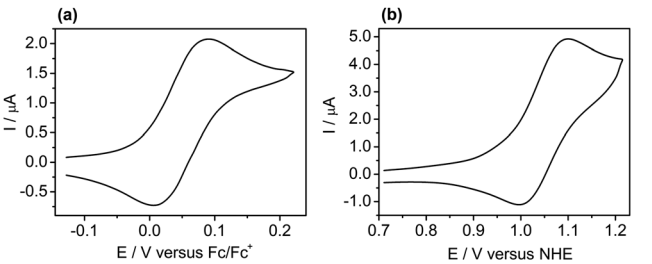

Fig. 4 The cyclic voltammograms of **1** at a scan rate of 25 mV s^{-1} (a) in acetonitrile solution (1 mM) with addition of NBu_4ClO_4 (1 M) and (b) in aqueous solution (1 mM) with addition of $NaClO_4$ (1 M) as supporting electrolyte.

Mn(IV) complexes soluble in water, like hexacyanomanganates[6a] and porphyrin complexes,[6b] undergo decomposition to MnO_2. Therefore, our findings open up a possibility for aqueous Mn(IV) chemistry, in particular, exploring rich redox chemistry of hydrazide clathrochelates and their potential use in redox catalysis.[13] The opportunities of *exo*-chelating coordination may result in obtaining polynuclear complexes and MOFs featuring building blocks with a paramagnetic center possessing an unusual electronic structure.

The project has received funding from the European Union's Horizon 2020 Research and Innovation Programme under the Marie Skłodowska-Curie grant agreement no. 778245. AOH and IOF acknowledge funding received from the Ministry of Education and Science of Ukraine (grant no. 19BF037-04). The high-field EPR spectra were recorded at the NHMFL, which is funded by the NSF through the Cooperative Agreement No. DMR-1644779, and the State of Florida. This research used resources of the Oak Ridge Leadership Computing Facility (OLCF), which is a DOE Office of Science User Facility supported under Contract DE-AC05-00OR22725.

Conflicts of interest

There are no conflicts to declare.

Notes and references

1 (*a*) Y. Z. Voloshyn, N. A. Kostromina and R. Krämer, *Clathrohelates: Synthesis, Structure and Properties*, Elsevier, Amsterdam, 2002; (*b*) Y. Voloshin, I. Belaya and R. Krämer, *Cage metal complexes: Clathrochelates revisited*, Springer, 2017.

2 S. Tomyn, S. I. Shylin, D. Bykov, V. Ksenofontov, E. Gumienna-Kontecka, V. Bon and I. O. Fritsky, *Nat. Commun.*, 2017, **8**, 14099.

3 (*a*) S. I. Shylin, M. V. Pavliuk, L. D'Amario, F. Mamedov, J. Sá, G. Berggren and I. O. Fritsky, *Chem. Commun.*, 2019, **55**, 3335–3338; (*b*) S. I. Shylin, M. V. Pavliuk, L. D'Amario, I. O. Fritsky and G. Berggren, *Faraday Discuss.*, 2019, **215**, 162–174.

4 (*a*) O. I. Artyushin, E. V. Matveeva, A. V. Vologzhanina and Y. Z. Voloshin, *Dalton Trans.*, 2016, **45**, 5328–5333; (*b*) O. A. Varzatskii, S. V. Shul'ga, A. S. Belov, V. V. Novikov, A. V. Dolganov, A. V. Vologzhanina and Y. Z. Voloshin, *Dalton Trans.*, 2014, **43**, 17934–17948; (*c*) G. E. Zelinskii, A. S. Belov, A. V. Vologzhanina, I. P. Limarev, P. V. Dorovatovskii, Y. V. Zubavichus, E. G. Lebed, Y. Z. Voloshin and A. G. Dedov, *Polyhedron*, 2019, **160**, 108–114; (*d*) Y. Z. Voloshin, O. A. Varzatskii, I. I. Vorontsov and M. Y. Antipin, *Angew. Chem., Int. Ed.*, 2005, **44**, 3400–3402; (*e*) Y. Z. Voloshin, V. V. Novikov, Y. V. Nelyubina, A. S. Belov, D. M. Roitershtein, A. Savitsky, A. Mokhir, J. Sutter, M. E. Miehlich and K. Meyer, *Chem. Commun.*, 2018, **54**, 3436–3439.

5 (*a*) V. A. Larson, B. Battistella, K. Ray, N. Lehnert and W. Nam, *Nat. Rev. Chem.*, 2020, **4**, 404–419; (*b*) M. M. Najafpour, I. Zaharieva, Z. Zand, S. Maedeh Hosseini, M. Kouzmanova, M. Hołyńska, I. Tranca, A. W. Larkum, J.-R. Shen and S. I. Allakhverdiev, *Coord. Chem. Rev.*, 2020, **409**, 213183; (*c*) M. M. Najafpour, G. Renger, M. Hołyńska, A. N. Moghaddam, E.-M. Aro, R. Carpentier, H. Nishihara, J. J. Eaton-Rye, J.-R. Shen and S. I. Allakhverdiev, *Chem. Rev.*, 2016, **116**, 2886–2936; (*d*) Y. Sheng, I. A. Abreu, D. E. Cabelli, M. J. Maroney, A.-F. Miller, M. Teixeira and J. S. Valentine, *Chem. Rev.*, 2014, **114**, 3854–3918; (*e*) R. Bonetta, *Chem. – Eur. J.*, 2018, **24**, 5032–5041.

6 (*a*) W. E. Buschmann, C. Vazquez, M. D. Ward, N. C. Jones and J. S. Miller, *Chem. Commun.*, 1997, 409–410; (*b*) C. Arunkumar, Y.-M. Lee, J. Y. Lee, S. Fukuzumi and W. Nam, *Chem. – Eur. J.*, 2009, **15**, 11482–11489.

7 (*a*) I. I. Creaser, L. M. Engelhardt, J. M. Harrowfield, A. M. Sargeson, B. Skelton and A. White, *Aust. J. Chem.*, 1993, **46**, 465–476; (*b*) P. A. Anderson, I. I. Creaser, C. Dean, J. M. Harrowfield, E. Horn, L. L. Martin, A. M. Sargeson, M. R. Snow and E. R. T. Tiekink, *Aust. J. Chem.*, 1993, **46**, 449–463; (*c*) J. Coyle, M. G. B. Drew, C. J. Harding, J. Nelson and R. M. Town, *J. Chem. Soc., Dalton Trans.*, 1997, 1123–1126.

8 (*a*) S. Jurisson, L. Francesconi, K. E. Linder, E. Treher, M. F. Malley, J. Z. Gougoutas and A. D. Nunn, *Inorg. Chem.*, 1991, **30**, 1820–1827; (*b*) W.-Y. Hsieh and S. Liu, *Inorg. Chem.*, 2006, **45**, 5034–5043; (*c*) C. Ge, J. Zhang, Z. Qin, P. Zhang, R. Zhang, H. Zhao, Y. Wang and X. Zhang, *Inorg. Chim. Acta*, 2017, **463**, 134–141; (*d*) Z. Ma, Y. Bai, L. Wang, C. Ge, H. Bian, S. Zhang and X. Zhang, *J. Mol. Struct.*, 2020, **1219**, 128481.

9 M. Llunell, D. Casanova, J. Cirera, P. Alemany and S. Alvarez, SHAPE, version 2.1, Universitat de Barcelona, Barcelona, Spain, 2013.

10 R. D. Shannon, *Acta Crystallogr., Sect. A: Cryst. Phys., Diffr., Theor. Gen. Crystallogr.*, 1976, **32**, 751–767.

11 (*a*) M. Zlatar, M. Gruden, O. Y. Vassilyeva, E. A. Buvaylo, A. N. Ponomarev, S. A. Zvyagin, J. Wosnitza, J. Krzystek, P. Garcia-Fernandez and C. Duboc, *Inorg. Chem.*, 2016, **55**, 1192–1201; (*b*) D. Premužić, M. Hołyńska, A. Ozarowski, C. Pietzonka, A. Roseborough and S. A. Stoian, *Inorg. Chem.*, 2020, **59**, 10768–10784.

12 (*a*) I. O. Fritsky, H. Kozłowski, O. M. Kanderal, M. Haukka, J. Świątek-Kozłowska, E. Gumienna-Kontecka and F. Meyer, *Chem. Commun.*, 2006, 4125–4127; (*b*) I. O. Fritsky, H. Kozłowski, P. J. Sadler, O. P. Yefetova, J. Świątek-Kozłowska, V. A. Kalibabchuk and T. Głowiak, *J. Chem. Soc., Dalton. Trans.*, 1998, **19**, 3269–3274.

13 S. Xu, L. Bucinsky, M. Breza, J. Krzystek, C.-H. Chen, M. Pink, J. Telser and J. M. Smith, *Inorg. Chem.*, 2017, **56**, 14315–14325.